Electrosynthesis and Characterization of Symmetrical and Unsymmetrical Linear Porphyrin Dimers and Their Precursor Monomers

A. Giraudeau, L. Ruhlmann, L. El Kahef, and M. Gross*

Contribution from the Laboratoire d'Electrochimie et de Chimie Physique du Corps Solide, URA au CNRS No. 405, Université Louis Pasteur, 4 rue Blaise Pascal, F-67000 Strasbourg, France

Received July 19, 1995. Revised Manuscript Received January 29, 1996[⊗]

Abstract: The electrochemical synthesis of linear symmetrical octaethylporphyrin−octaethylporphyrin and unsymmetrical tetraphenylporphyrin−octaethylporphyrin dimeric porphyrins with one viologen as a spacer and of their precursor porphyrin monomers is reported. The mechanism of the electrochemical substitution leading to the dimeric porphyrins is discussed. These new compounds have been characterized by ^{1}H NMR, UV−vis spectroscopy, FAB mass spectroscopy, and microanalysis. Electrochemical data are reported, and the redox behavior is analyzed for the monomers and the dimers in terms of $\pi-\pi$ interactions between the two porphyrin centers. ESR measurements were carried out on the unsymmetrical Cu−Zn and Cu−Cu dimeric metalloporphyrins which displayed intermolecular metal interactions.

Introduction

Many chemical models have been built in the past years aimed at mimicking natural photosynthetic systems.[1] Among these, polynuclear porphyrins and phthalocyanines attracted considerable interest owing to the wide diversity of their electron transfer characteristics in relation with their chemical structure.[2] Of these characteristics, electronic coupling between the monomeric subunits in supramolecules is of major interest because of its relevance to intramolecular electron transfer in donor−acceptor couples.[3] The effects of the intervening matrix on this electronic coupling have been scrutinized[4] in molecules incorporating both electron donor and electron acceptor sites, and consistent trends emerged. First, when the donor and the acceptor were covalently linked through a rigid spacer, the electron transfer rates were enhanced via through-bond coupling. Second, the decrease of the electron transfer rate with the distance between the donor and the acceptor was more important with aliphatic than aromatic spacers. For instance, poly(phenylene)-bridged bisporphyrin adducts[5] exhibited slower intramolecular electron transfer rates which depended little on the increasing distance between the donor−acceptor pairs but which reflected, instead, disruption of electronic coupling by the twist angles at each phenyl−porphyrin connection.[6] Important information on the electronic interactions between donor and acceptor moieties in polyporphyrin molecules[7,8] emerged from correlations between their redox and optical properties. L'Her, Collman, et al.[9] demonstrated that the coupling of two porphyrins in a cofacial configuration induced a "cofacial effect" which originated in strong interactions between the two π-electron ring systems. These authors were able to modulate the extent of this "cofacial effect" by modifying the chemical

[⊗] Abstract published in *Advance ACS Abstracts,* March 1, 1996.

(1) (a) Deisenhofer, J.; Epp, O.; Miki, K.; Huber, R.; Michel, H. *J. Mol. Biol.* **1984**, *180*, 385−398. (b) Deisenhofer, J.; Michel, H. *Angew. Chem., Int. Ed. Engl.* **1989**, *28*, 829−847. (c) Boxer, S. G. *Biochim. Biophys. Acta* **1983**, *726*, 265−292. (d) Wasielewski, M. R. *Photochem. Photobiol.* **1988**, *47*, 923−929. (e) Gust, D.; Moore, T. A. *Science* **1989**, *244*, 35−41. (f) Huber, R. *Angew. Chem., Int. Ed. Engl*. **1989**, *28*, 848−869. (g) Akins, L.; Guo, C. *Adv. Mater.* **1994**, *6*, 512−516.

(2) (a) Bixon, M.; Fajer, J.; Feher, G.; Freed, J. H.; Gamliel, D.; Hoff, A. J.; Levanon, H.; Möbius, K.; Nechushtai, R.; Norris, J. R.; Scherz, A.; Sessler, J. L.; Stehlik, D. *Isr. J. Chem.* **1992**, *32*, 449−467. (b) Miller, J. R.; Beitz, J. V.; Huddleston, R. K. *J. Am. Chem. Soc.* **1984**, *106*, 5057−5068. (c) Penfield, K. W.; Miller, J. R.; Paddon-Row, M. N.; Cotsaris, E.; Oliver, A. M.; Hush, N. S. *J. Am. Chem. Soc.* **1987**, *109*, 5061−5065. (d) Closs, G. L.; Miller, J. R. *Science* **1988**, *240*, 440−447. (e) Oevering, H.; Verhoeven, J. W.; Paddon-Row, M. N.; Costaris, E.; Hush, N. S. *Chem. Phys. Lett.* **1988**, *143*, 488−495. (f) Schwartz, F. P.; Gouterman, M.; Muljiani, Z.; Dolphin, D. *Bioinorg. Chem.* **1972**, *2*, 1−32. (g) Heitele, H.; Michel-Beyerle, M. E. *J. Am. Chem. Soc.* **1985**, *107*, 8286−8288.

(3) (a) Closs, G.; Calcaterra, L.; Green, N.; Penfield, K.; Miller, J. R. *J. Phys. Chem.* **1986**, *90*, 3673−3683. (b) Warman, J.; Haas, M.; Paddon-Row, M. N.; Costaris, E.; Hush, N.; Verhoeven, J. *Nature* **1986**, *320*, 615. (c) Sessler, J. L.; Johnson, M. R.; Lin, T. Y.; Creager, S. *J. Am. Chem. Soc.* **1988**, *110*, 3659−3661. (d) Sessler, J. L.; Johnson, M. R.; Creager, S. E.; Fettinger, J. C.; Ibers, J. A. *J. Am. Chem. Soc.* **1990**, *112*, 9310−9329. (e) Sessler, J. L.; Wang, B.; Harriman, A. *J. Am. Chem. Soc.* **1995**, *117*, 704−714. (f) Brun, A. M.; Harriman, A.; Heitz, V.; Sauvage, J. P. *J. Am. Chem. Soc.* **1991**, *113*, 8657−8663. (g) Brun, A. M.; Atherton, S. J.; Harriman, A.; Heitz, V.; Sauvage, J. P. *J. Am. Chem. Soc.* **1992**, *114*, 4632−4639.

(4) (a) Osuka, A.; Furuta, H.; Maruyama, K. *Chem. Lett.* **1986**, 479−482. (b) Osuka, A.; Maruyama, K.; Hirayama, S. *Tetrahedron* **1989**, *45*, 4815−4830. (c) Osuka, A.; Maruyama, K.; Mataga, N.; Asahi, T.; Yamazaki, I.; Tamai, N. *J. Am. Chem. Soc.* **1990**, *112*, 4958−4959.

(5) (a) Finck, P.; Heitele, H.; Michel-Beyerle, M. E. *J. Phys. Chem.* **1988**, *92*, 6584−6590. (b) Miller, J. R.; Beitz, J. *J. Chem. Phys.* **1981**, *74*, 6746−6756.

(6) (a) Helms, A.; Heiler, D.; McLendon, G. *J. Am. Chem. Soc.* **1992**, *114*, 6227−6238. (b) Helms, A.; Heiler, D.; Mc Lendon, G. *J. Am. Chem. Soc.* **1991**, *113*, 4325−4327. (c) Mc Lendon, G. *Acc. Chem. Res.* **1988**, *21*, 160−167.

(7) (a) Hemdrecher, H. K.; Lüdtke, K. *Tetrahedron* **1993**, *42*, 9489−9494. (b) Pandey, R. K.; Forsyth, T. P.; Gerzevske, K. R.; Lin, J. J.; Smith, K. M. *Tetrahedron Lett.* **1992**, *33*, 5315−5318. (c) Hammel, D.; Eak, P.; Schuler, B.; Heinze, J.; Mülen, K. *Adv. Mater.* **1992**, *4*, 737−739. (d) Lin, V. S.-Y.; Di Magno, S. G.; Therien, M. J. *Science* **1994**, *264*, 1105−1111. (e) Anderson, H. L. *Inorg. Chem.* **1994**, *33*, 972−981. (f) Anderson, S.; Anderson, H. L.; Sanders, J. K. M. *Acc. Chem. Res.* **1993**, *26*, 469−475. (g) Cosper, J. J.; Ali, M. *J. Chem. Soc., Chem. Commun.* **1994**, 1707−1708. (h) Arnold, D. P.; Heath, G. A. *J. Am. Chem. Soc.* **1993**, *115*, 12197−12198. (i) Arnold, D. P.; Nitschinck, L. J. *Tetrahedron Lett.* **1993**, *34*, 693−696. (j) Crossley, M. J.; Burn, P. L. *J. Chem. Soc., Chem. Commun.* **1991**, 1569−1571. (k) Lü, T. X.; Reimers, J. R.; Crossley, M. J.; Hush, N. S. *J. Phys. Chem.* **1994**, *98*, 11878−11884.

(8) (a) Osuka, A.; Nagata, T.; Maruyama, K. *Chem. Lett.* **1991**, 1687−1690. (b) Tamiaki, H.; Suzuki, S.; Maruyama, K. *Bull. Chem. Soc. Jpn.* **1993**, *66*, 2633−2697. (c) Osuka, A.; Nakajima, S.; Maruyama, K.; Mataga, N.; Asahi, T.; Yamazaki, I.; Nishimura, Y.; Ohno, T.; Nazaki, K. *J. Am. Chem. Soc.* **1993**, *115*, 4577−4589. (d) Osuka, A.; Kobayashi, F.; Maruyama, K.; Mataga, N.; Asahi, T.; Okada, T.; Yamazaki, I.; Nishimura, Y. *Chem. Phys. Lett.* **1993**, *201*, 223−228.

(9) Le Mest, Y.; L'Her, M.; Hendricks, N. H.; Kim, K.; Collman, J. P. *Inorg. Chem.* **1992**, *31*, 835−847.

0002-7863/96/1518-2969$12.00/0

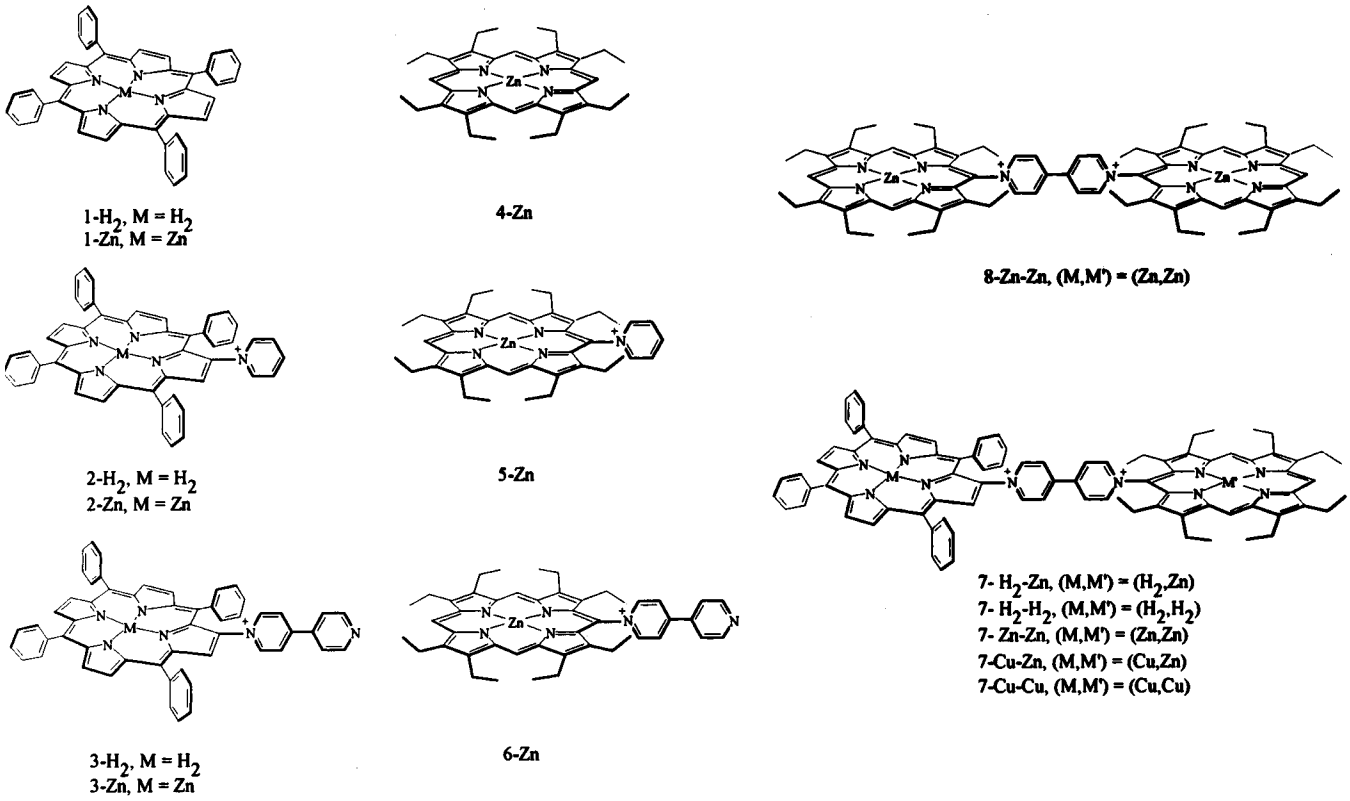

Figure 1. Porphyrins and bisporphyrins investigated in this study.

nature and length of the linking bridge. This modulation was monitored via the gradual uncoupling of the oxidation and reduction steps characteristic of the porphyrins in the dimer and also through changes in the UV−vis absorption spectra observed upon generation of cation radicals. In other porphyrin dimers, Sessler et al.[3d] ascribed shifts and/or splittings of the UV−vis bands to excitonic interactions between the porphyrin π systems: the effects being more pronounced in gabled than in linear dimers. The general trend among the various models studied was that interactions between two porphyrins subunits of a given dimer induced shifts and/or splittings of the UV−vis absorption bands.

Our interest in the electrochemical synthesis of porphyrin dimers was prompted by studies on the reactivity[10,11] of porphyrin π-cation radicals with nucleophiles. It was observed[12ab] that electrochemical oxidation of zinc tetraphenylporphyrin in the presence of nucleophiles generated stable β-substituted porphyrins. The yields of this simple one-pot reaction were quite good (>60%). It was therefore reasonable to expect that this method might also be effective for the synthesis of bisporphyrins from porphyrin monomers and an appropriate nucleophile as spacer. A Lewis base containing two distinct nucleophilic sites was considered as a good spacer, on the assumption that each of the two sites might react with one porphyrin. Therefore, the electrochemical oxidation of meso-tetraphenylporphyrin (TPP) or octaethylporphyrin (OEP) was carried out in the presence of 4,4′-bipyridine.

This reaction produced first β- or meso-substituted porphyrins for TPPs and OEPs, respectively. These resulting monomeric porphyrins, bearing 4,4′-bipyridinium as substituent, were, in turn, the precursors in the synthesis of the porphyrin dimers. In the next phase, the precursors also reacted as nucleophiles with electrogenerated oxidized porphyrins to generate the expected bisporphyrins.

This paper reports the electrosynthesis of symmetric (OEP−OEP) and asymmetric (OEP−TPP) linear porphyrin dimers. The mechanism of this reaction is discussed. The redox characteristics of the porphyrin dimers and their UV−vis absorption spectra have been analyzed to identify the interactions between the two porphyrin moieties in the dimer. Proton NMR spectra allowed unambiguous assignment of the different substitutions and showed rotation between the two porphyrin rings in the bisporphyrins. An asymmetric Cu−Cu dimer was also prepared to provide a good ESR sensor for detecting metal−metal interactions. The porphyrins investigated are illustrated in Figure 1.

Electrosynthesis

Precursor Monomers. 1. (H_2TPP-β-4,4′-bpy)$^+ClO_4^-$ (3-H_2). The first oxidation step of H_2TPP (**1**-H_2) was a reversible[13] one-electron reaction in CH_3CN:1,2-$C_2H_4Cl_2$ (1:4) (Figure 2), and it became an irreversible two-electron process in the presence of the nucleophile pyridine. Under the latter conditions, exhaustive electrooxidation generated the corresponding β-substituted porphyrin **2**-H_2.[12c]

(10) (a) Felton, R. H. In *The Porphyrins*; Dolphin, D., Ed.; Academic Press: New York, 1979; Vol. 5, Chapter 3. (b) Dolphin, D.; Felton, R. H. *Acc. Chem. Res.* **1974**, *7*, 26−32. (c) Stanienda, A. *Z. Phys. Chem.* **1964**, *229*, 259−266. (d) Wolberg, A.; Manassen, J. *J. Am. Chem. Soc.* **1970**, *92*, 2982−2991. (e) Carnieri, N.; Harriman, A. *Inorg. Chim. Acta* **1982**, *62*, 103−107. (f) Spaulding, L. O.; Eller, P. G.; Bertrand, J. A.; Felton, R. H. *J. Am. Chem. Soc.* **1974**, *96*, 982−987.

(11) (a) Dolphin, D.; Muljiani, Z.; Rousseau, K.; Borg, D. C.; Fajer, J.; Felton, R. H. Ann. N. Y. *Acad. Sci.* **1973**, *206*, 117−119. (b) Barnett, G. H.; Smith, K. M. *J. Chem. Soc., Chem. Commun.* **1974**, 772−773. (c) Barnett, G. H.; Evans, B.; Smith, K. M. *Tetrahedron Lett.* **1976**, *44*, 4009−4012. (d) Padilla, A. G.; Wu, S. M.; Shine, H. J. *J. Chem. Soc., Chem. Commun.* **1976**, 236−237. (e) Shine, H. J.; Padilla, A. G.; Wu, S. M. *J. Org. Chem.* **1979**, *44*, 4069−4075. (f) Rachlewicz, K.; Latos-Grazynski, L. *Inorg. Chem.* **1995**, *34*, 718−727.

(12) (a) El Kahef, L.; El Meray, M.; Gross, M.; Giraudeau, A. *J. Chem. Soc., Chem. Commun.* **1986**, 621−622. (b) Giraudeau, A.; El Kahef, L. *Can. J. Chem.* **1991**, *69*, 1161−1165. (c) El Kahef, L.; Gross, M.; Giraudeau, A. *J. Chem. Soc., Chem. Commun.* **1989**, 963.

(13) Stanienda, A. *Z. Naturforsch.* **1968**, *23b*, 147−152.

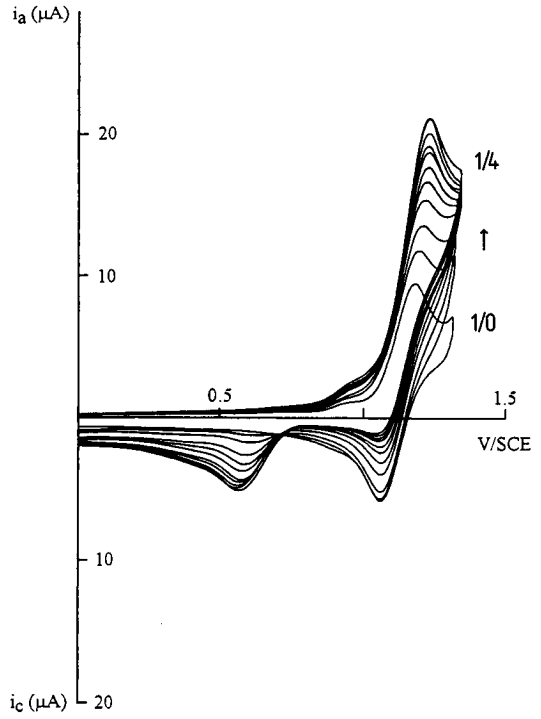

Figure 2. Cyclic voltammetry changes observed in the first-oxidation step of H_2TPP after addition of pyridine. CH_3CN + 1,2-$C_2H_4Cl_2$ (1/4) + 0.1 M TEAP. v = 100 mV s^{-1}. Working electrode: Pt. Relative concentrations [H_2TPP]/[pyridine]: 1/0−1/4.

Similar results were obtained in the oxidation of H_2TPP in the presence of 4,4′-bipyridine as nucleophile. In a typical experiment, 30 mg (0.049 mmol) of H_2TPP (**1**-H_2) and 150 mg (0.960 mmol) of 4,4′-bipyridine were introduced in 25 mL of the mixed solvent CH_3CN:$CHCl_3$ (1:4) containing 0.1 M TEAP (tetraethylammonium perchlorate). The working electrode potential was held constant at 1.05 V/SCE, and the initial violet solution turned increasingly yellow-brown. During the electrolysis, the solution was monitored by UV−vis spectrophotometry. The decrease of the oxidation current was not exponential with time. When this current reached the residual current measured in the absence of electroactive material, typically after 3 h, in the above conditions, the number of electrons transferred was 2.2/molecule of H_2TPP. After extraction and purification (see the Experimental Section), the β-substituted porphyrin (H_2TPP-β-4,4′-bpy)$^+ClO_4^-$ (**3**-H_2) was characterized, and the yield was 94% for the following global reaction:

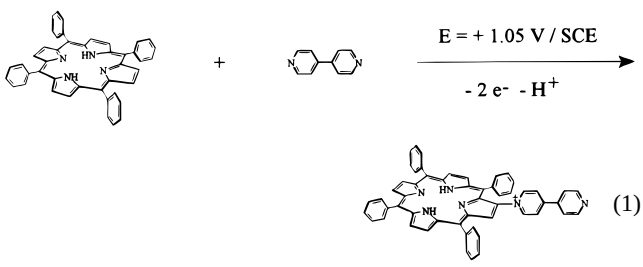

(1)

2. (ZnOEP-meso-py)$^+ClO_4^-$ (5-Zn). In a first set of experiments, the electrochemical oxidation of ZnOEP was monitored in the presence of the nucleophile pyridine. The purpose was to determine whether the experimental conditions used for the electrooxidative β-substitution on ZnTPP in the presence of pyridine[12a,b] were also valid for meso-substitution of ZnOEP.[14] The product of the electrolysis was isolated and characterized as the meso-substituted zinc porphyrin (ZnOEP-meso-py)$^+ClO_4^-$(**5**-Zn), with 71% yield.

3. (ZnOEP-meso-4,4′-bpy)$^+ClO_4^-$ (6-Zn). Stationary and cyclic voltammetry revealed identical characteristics for the ZnOEP oxidation in the presence of 4,4′-bipyridine and pyridine. After electrolyzing for 48 h, the initial pink solution turned violet and finally yellow-brown. The purified (ZnOEP-meso-4,4′-bpy)$^+ClO_4^-$ (**6**-Zn) was obtained with 78% yield, the global reaction being as follows:

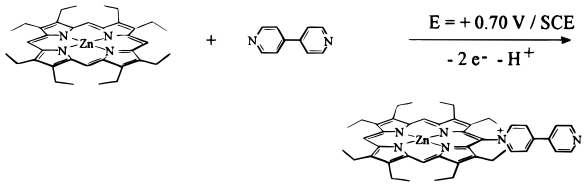

(2)

In all cases, protons are liberated during the course of the reaction and should be trapped by the added Lewis base to prevent demetalation of the metalloporphyrin. The minimum required is 2 equiv of the Lewis base. When oxidized the free base H_2TPP protonated easily, and therefore the Lewis base was added in a large excess to prevent formation of inactive H_4TPP^{2+}. When the porphyrin P is oxidized in the presence of 4,4′-bipyridine, the reaction is limited to the formation of the monomeric P-bpy$^+$ because the 4,4′-bipyridine present in solution acted as a stronger nucleophile than the generated P-bpy$^+$.

Dimers. 1. (H_2TPP-β-4,4′-bpy-meso-ZnOEP)$^{2+}2ClO_4^-$ (7-H_2-Zn). The β-substituted free base porphyrin **3**-H_2 reacted as nucleophile toward electrochemically generated ZnOEP$^{\bullet+}$ cation radicals. ZnOEP (**4**-Zn) was choosen here because its oxidation potential is lower ($E_{1/2}$ = 0.68 V/SCE) than that of the β-substituted free base **3**-H_2 ($E_{1/2}$ = 1.25 V/SCE), and therefore the electrogeneration of ZnOEP$^{\bullet+}$ was possible without oxidation of **3**-H_2. After electrolyzing **4**-Zn for 48 h in the presence of **3**-H_2, the dimer **7**-H_2-Zn, namely, (H_2TPP-β-4,4′-bpy-meso-ZnOEP)$^{2+}2ClO_4^-$, was obtained with 73% yield, according to the following global reaction scheme:

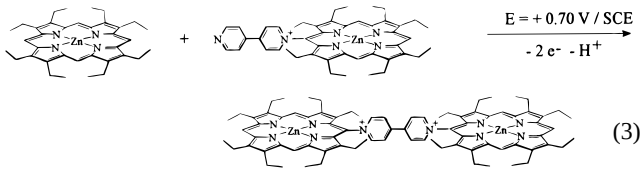

(3)

2. (ZnOEP-meso-4,4′-bpy-meso-ZnOEP)$^{2+}2ClO_4^-$ (8-Zn-Zn). Because the difference between the oxidation potentials of **4**-Zn and of **6**-Zn is 230 mV (Table 1), the electrolysis potential had to be held strictly constant at 0.70 V/SCE, which is as low as possible to avoid the first oxidation of the nucleophile **6**-Zn ($E_{1/2}$ = 0.91 V/SCE) and nevertheless to generate ZnOEP$^{\bullet+}$ at an appreciable rate from **4**-Zn ($E_{1/2}$ = 0.68 V/SCE, Table 1). After 72 h of electrolysis, the dimer **8**-Zn-Zn was obtained with 68% yield, according to the following reaction scheme:

(14) (a) Callot, H. J.; Louati, A.; Gross, M. *Tetrahedron Lett.* **1980**, *21*, 3281−3284. (b) Callot, H. J.; Louati, A.; Gross, M. *Bull. Soc. Chim. Fr.* **1983**, 317−320.

Table 1. Electrochemical Data for the Studied Porphyrins and Bisporphyrins[a]

	ring oxidation					ring reduction		
porphyrin	$E_{1/2}^{III}$	$E_{1/2}^{II}$	$E_{1/2}^{I}$			$E_{1/2}^{I}$	$E_{1/2}^{II}$	$E_{1/2}^{III}$
H_2TPP		*1.34*	*1.10*			*−1.10*	*−1.48*	
ZnTPP		*1.16*	*0.80*			*−1.37*	*−1.75*	
CuTPP		*1.19*	*0.79*			*−1.46*		
H_2OEP[d]		1.30	0.81			−1.46	−1.86	
ZnOEP		0.94	0.68			−1.60		
CuOEP[d]		1.19	0.79			−1.46		
				py$^+$ or 4,4′-bpy$^+$ Reduction				
2-H_2			*1.19*[b,c]	**−0.96**		−1.14[c]		
2-Zn		*1.29*	*0.96*	−1.06[c]		*−1.38*		
5-Zn		1.27	0.94	**−1.10**		−1.60		
3-H_2			*1.25*[c]	**−0.73**		*−1.12*	*−1.40*	
3-Zn		*1.25*	*0.96*	**−0.72**		*−1.26*		
6-Zn		1.20[c]	0.91	**−0.65**		−1.31		
				Viologen Reduction				
7-H_2-H_2		*1.34*[c]	**1.20**[b]	***−0.05***	***−0.50***	*−1.15*	**−1.32**[b]	
7-H_2-Zn	*1.27*[c]	1.22[b]	0.93	***−0.06***	***−0.59***	*−1.18*	*−1.41*	−1.60
7-Zn-Zn		**1.27**[b]	**0.95**[b]	***−0.10***	***−0.64***	*−1.35*		
7-Cu-Zn	*1.43*	**1.18**[b]	0.92	***−0.08***	***−0.63***	*−1.32*	**−1.67**[b]	
7-Cu-Cu	**1.42**[b]	*1.16*	1.07	***−0.05***	***−0.58***	*−1.31*	−1.47	**−1.66**[b]
8-Zn-Zn		1.22[b]	0.90[b]	***−0.06***	***−0.63***	*−1.65*		

[a] All potentials in V/SCE obtained from stationary (RDE) voltammetry in $CH_3CN/1,2\text{-}C_2H_4Cl_2$ (1:4) and 0.1 M TEAP. Working electrode: Pt. Potential values in italics were observed for TPP; normal characters for OEP and underlined potentials were observed in both OEP and TPP systems. All steps were reversible one-electron transfers except those with b and c superscripts. [b] Two-electron transfer. [c] Irreversible transfer. [d] Reference 34b.

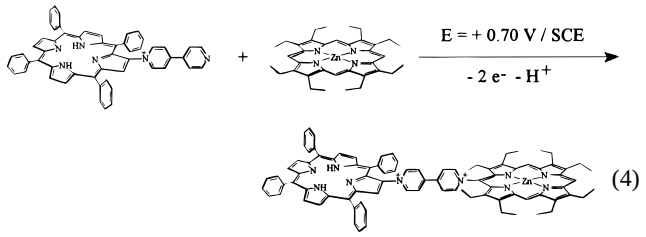

(4)

Selective Metalation of the Unsymmetrical Dimer TPP−OEP (7-H_2-H_2). This dimer was obtained by demetalation of **7**-H_2-Zn with HCl/acetone. Zn was incorporated into the β-substituted free base **3**-H_2 by the usual reaction of zinc acetate with free base in methanol/chloroform solution to yield **3**-Zn. Similarly, symmetrical (homo-dimetalated) **7**-Zn-Zn was obtained by reaction of **7**-H_2-H_2 free base with excess zinc acetate, and **7**-Cu-Cu with excess copper acetate. As well, the hetero-dimetalated **7**-Cu^{II}-Zn bisporphyrin was obtained by reaction of **7**-H_2-Zn with 1.1 equiv of $Cu^{II}(CH_3COO)_2 \cdot 2H_2O$ in CH_2Cl_2/CH_3OH. The acetate counterions of the metalloporphyrins were converted to perchlorate by treatment with tetraethylammonium perchlorate in order to have a homogeneous series of complexes.

Reaction Mechanisms

Previous results[12b] on TPP have established that the substitution of a nucleophile (Nu) on a porphyrin (P_1) was achieved in a two-electron reaction involving two chemical steps, a deprotonation and a nucleophilic substitution:

$$P_1 + 2Nu \xrightarrow{E_1^{ox}} P_1\text{-}\beta\text{-}Nu^+ + 2e^- + NuH^+$$

In the present electrosynthesis of the precursor monomers and dimers, this reaction was validated as a global reaction scheme. Because a proper understanding of the mechanism of these oxidations allows the reactions conditions to be tailored so as to obtain specific products in both a useful and practical manner, we attempted to understand the mechanism in detail. With the alkyl-substituted benzenes, the mechanism[15] is apparent from the nature of the products obtained. Nucleophilic substitutions result from an EC_NEC_B process, and side-chain substitutions result from an EC_BEC_N scheme.[16] With the other substrates the distinction is not as readily apparent.

In the presence of nucleophiles like pyridine, ZnOEP and ZnTPP exhibited similar first-oxidation curves in stationary and cyclic voltammetry. The free base H_2TPP exhibited a specific, distinct behavior. Therefore the first oxidation of H_2TPP and ZnTPP was studied, and pyridine was selected as nucleophile because of the easy availability of its derivatives. The only effect of added pyridine on the oxidation of ZnTPP was that the first-oxidation potential, which corresponded to the generation of the radical monocation, was shifted toward more negative potentials,[17] as expected from the axial coordination of pyridine on the central metal. In order to establish the reaction mechanism of the oxidative nucleophilic substitution, a series of exhaustive electrolytic oxidations were therefore carried out on ZnTPP (first oxidation) in the presence of several substituted pyridines[18] displaying a wide range of Lewis basicities. In the presence of 3-picoline (3-pic) and 3,5-lutidine (3,5-lut), the oxidation products were β-substituted porphyrins (ZnTPP-β-3-pic)$^+$ and (ZnTPP-β-3,5-lut)$^+$ and required 2 Faradays/mol of substituted porphyrin. In the presence of 2-picoline, 2,6-lutidine, 3-bromopyridine, or 4-cyanopyridine, the cation radical ZnTPP$^{\bullet+}$ [19] was the sole product of the oxidation. These experiments indicated clearly that, with nucleophiles whose pK_a was close to that of the pyridine, the nucleophilic substitution did not occur when the ortho carbons (2 or 6) of the pyridine were sterically crowded or when the pK_a of the nucleophile was low.

(15) Adams, R. N. *Electrochemistry at Solid Electrodes*; M. Dekker: New York, 1969; Chapter 10.

(16) Mechanism is EC_NEC_B when the initially formed cation radical $R^{\bullet+}$ is captured by a nucleophile, and ring substitution is the ultimate result. Mechanism is EC_BEC_N when $R^{\bullet+}$ transfers first a proton to a base, and the ultimate result is side-chain substitution.

(17) (a) Manassen, J. *Isr. J. Chem.* **1974**, *12*, 1059−1067. (b) Giraudeau, A.; Gross, M.; Callot, H. J. *Electrochim. Acta* **1981**, *26*, 1839−1843. (c) Kadish, K. M.; Shine, L. R.; Rhodes, R. K.; Bottomley, L. A. *Inorg. Chem.* **1981**, *20*, 1274−1277. (d) Kadish, K. M.; Lin, X. Q.; Han, B. C. *Inorg. Chem.* **1987**, *26*, 4161−4167.

(18) (a) Schoefield, K. S. *Hetero-Aromatic Nitrogen Compounds*; Plenum Press: New York, 1967; p 146. (b) *Handbook of Chemistry and Physics*, 67th ed.; Weast, R. C., Ed.; CRC Press: Boca Raton, FL, 1986−1987; D. 159, 160.

They suggested therefore that the first chemical reaction was a nucleophilic attack rather than a deprotonation.

At variance with ZnTPP, the first-electrochemical oxidation curves of H_2TPP were modified in the presence of Lewis base nucleophiles.[20] When increasing amounts of pyridine were added to a solution of H_2TPP, the first-oxidation wave, observed by stationary voltammetry, increased at the expense of the second-oxidation wave. Ultimately, the first-oxidation wave exhibited a limiting current that was 2 times the current in the absence of pyridine, while the second-oxidation wave disappeared, at a pyridine concentration 4 times that of H_2TPP. Consistent with this result, the first-oxidation peak in cyclic voltammetry changed from a one-electron reversible signal to an irreversible one, while the peak current doubled and the second-oxidation peak disappeared (Figure 2). The method allowing this discrimination between an EC_N EC_B or EC_B EC_N scheme was described by Eberson and Parker.[21] It was based on monitoring the disappearance of the reduction peak of the cation radical $P^{\bullet+}$ upon addition of several pyridines having similar basicities but differing by the size and the positions of the substituents. The experimental scheme was as follows: All other experimental parameters being held constant, a first set of experiments established the concentration of pyridine (C_{py}) that was necessary to eliminate the reduction peak of $H_2TPP^{\bullet+}$. Under the same experimental conditions, elimination of this reduction peak required $4C_{py}$ with 2,6-lutidine, $2.5C_{py}$ with 2,4-lutidine, and only $2C_{py}$ with 3,5-lutidine. These results clearly show that a nucleophilic attack is the primary chemical step and not an acid−base reaction.

These results led to the following proposed mechanism:

$$\text{MTPP} \rightarrow \text{MTPP}^{\bullet+} + e^- \qquad (E_1)$$

$$\text{MTPP}^{\bullet+} + \text{Nu} \rightarrow (\text{MTPP-}\beta\text{-Nu})^{\bullet+} \qquad (C_N)$$

$$(\text{MTPP-}\beta\text{-Nu})^{\bullet+} \rightarrow (\text{MTPP-}\beta\text{-Nu})^{2+} + e^- \qquad (E_2)$$

$$(\text{MTPP-}\beta\text{-Nu})^{2+} \rightarrow (\text{MTPP-}\beta\text{-Nu})^{+} + H^+ \qquad (C_B)$$

When cyclic voltammetry was carried out on H_2TPP, new peaks were observed after addition of pyridine (Figure 3). Peak a at −0.38 V/SCE was ascribed[22] to the reduction of the cation py-H^+ to py and $^1/_2H_2$, while peak b at −0.25 V/SCE was assumed to correspond to the oxidation of the molecular hydrogen generated through peak a in the presence of a Lewis base. This proposed interpretation of peaks a and b implied that the pyridine nucleophile not only reacted with the porphyrin radical cation but that it was also acting as a Brönsted base in solution. When the rate of the nucleophilic reaction C_N was slow enough, only the first electron transfer was observed[23] on the CV or SV curves, as, for instance, with ZnTPP. The faster nucleophilic reaction (C_N) on the free base cation radical $H_2TPP^{\bullet+}$ may be explained by the higher reactivity of this radical. With ZnOEP, the reaction mechanism was the same ($E_1C_NE_2C_B$) as with ZnTPP, the only difference being that the substitution occurred at the meso-carbons of the porphyrin.

These results were consistent with those observed by Shine[11d,e] and Smith[11b,c] on the cation radicals $ZnTPP^{\bullet+}$ and $ZnOEP^{\bullet+}$ in the presence of pyridine. Two types of π-cation radicals have been reported for metalloporphyrins.[10b,f] Large spin density at the bridging meso-carbon atoms and small spin density at the pyrrole carbon atoms are characteristic of a_{2u} radicals, while a_{1u} radicals have nodes at the meso-carbons. Hence β-substitution is expected with a_{2u} radicals and meso-substitution with a_{1u} radicals as observed, respectively, with TPP and OEP π-cation radicals. Dolphin et al.[24] have also performed such β-substitutions with the cation radical $ZnTPP^{\bullet+}$ and the dication $ZnTPP^{2+}$. In the experiments reported here, electrogeneration of the dication from ZnTPP in the presence of pyridine did not produce such substitutions: Only an isoporphyrin was obtained, as previously reported by Kadish et al.[23] This isoporphyrin was characterized by its UV−vis absorption spectrum.[25] Results by Shine[11e] indicated that nitrite anions (NO_2^-) reacted on both the β- and the meso-positions of cation radical $ZnTPP^{\bullet+}$. Recent work[11f] demonstrated that pyridine β-substitutions occurred in iron tetraphenylporphyrin π-cation radical to give the stable β-substituted porphyrin and also the unstable isoporphyrin generated by attack of the pyridine at the meso- carbon. In our experiments, the presence of peak c on the CV curves (Figure 3) could be explained by reduction of such an isoporphyrin. Similar reductions steps[25b,c] characterized the redox chemistry of isoporphyrins. In these electrochemical substitutions carried out on tetraphenylporphyrins, the two pathways (β- and meso-attack) would occur, but only the β-attack leads to a stable configuration. This diverse reactivity of pyridine nucleophiles with porphyrin cation radicals may be rationalized on the basis of the views developed by Abrahamovitch et al.,[26] on the effects of the nucleophilic character of the reactant on to the reaction orientation. On this basis, it was expected that, in the presence of strong nucleophiles like pyridine, the electron densities at each carbon of the porphyrin cation radical determined the substitution site. In contrast, with weak nucleophiles, the

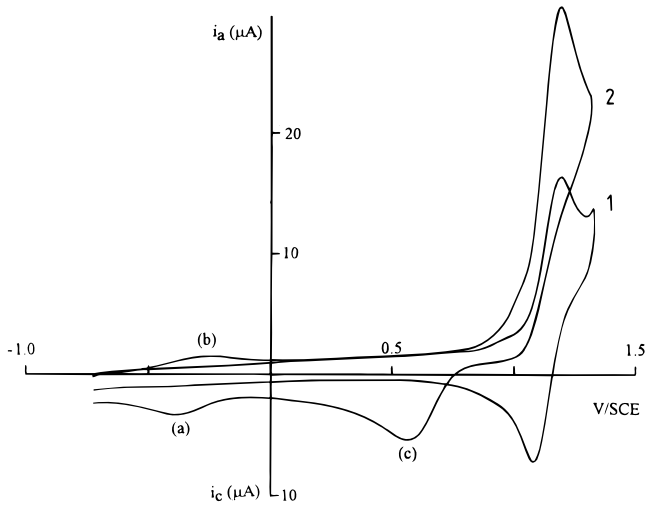

Figure 3. Effects of adding excess pyridine on the cyclic voltammogram of H_2TPP. CH_3CN + 1,2-$C_2H_4Cl_2$ (1/4) + 0.1 M TEAP. (1) H_2TPP, (2) H_2TPP + excess pyridine, after several cycles. υ = 100 mV s^{-1}. Working electrode: Pt. (a) py-H^+ + e^- ⇄ py + $^1/_2H_2$, (b) $^1/_2H_2$ ⇄ H^+ + e^-, (c) Reference 25.

(19) Fajer, J.; Borg, D. C.; Forman, A.; Dolphin, D.; Felton, R. H. *J. Am. Chem. Soc.* **1970**, *92*, 3451−3459.
(20) Lexa, D.; Reix, M. *J. Chem. Phys.* **1974**, *71*, 511−516.
(21) Parker, V. D.; Eberson, L. *Tetrahedron Lett.* **1969**, *33*, 2839−2842.
(22) Cauquis, G.; Cros, J. L.; Genies, M. *Bull. Soc. Chim. Fr.* **1971**, 3765−3772.
(23) Kadish, K. M.; Rhodes, R. K. *Inorg. Chem.* **1981**, *20*, 2961−2966.
(24) Dolphin, D.; Halko, D. J.; Johnson, E. C.; Rousseau, K. In *Porphyrin Chemistry Advances*; Longo, F. R., Ed.; Ann Arbor Science: MI, 1979; Chapter 10.
(25) (a) Dolphin, D.; Felton, R. H.; Borg, D. C.; Fajer, J. *J. Am. Chem. Soc.* **1970**, *92*, 743−745. (b) Hinman, A. S.; Pavelich, B. J.; Pons, S.; Kondo, A. E. *J. Electroanal. Chem.* **1987**, *234*, 145−162. (c) El-Kasmi, A.; Lexa, D.; Maillard, P.; Momenteau, M.; Saveant, J. M. *J. Am. Chem. Soc.* **1991**, *113*, 1586−1595.
(26) Abrahamovitch, R. A.; Sara, J. G. In *Advances in Heterocyclic Chemistry*; Katritzky, A. R., Boulton, A. J., Eds.; Academic Press: New York, 1966; Vol. 6.

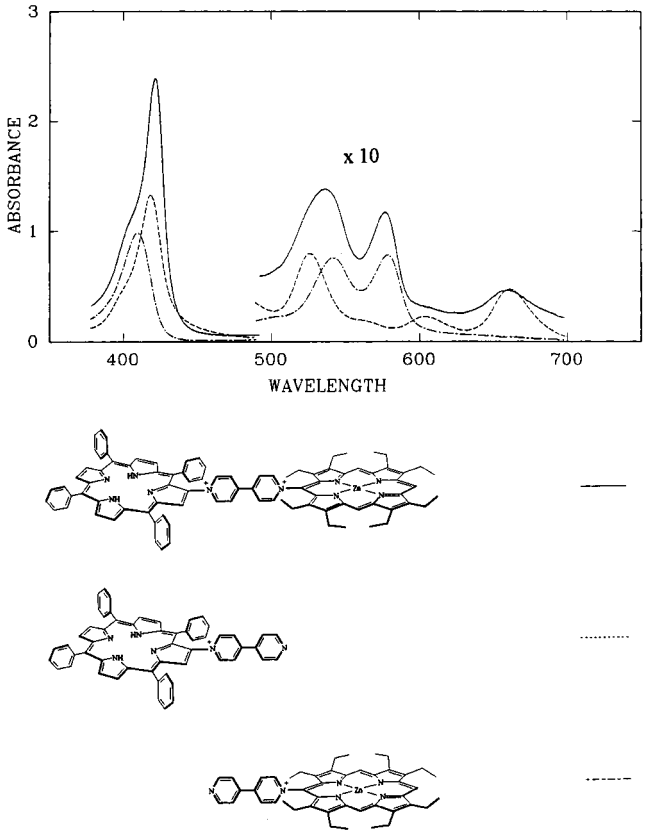

Figure 4. UV−vis absorption spectra of the bisporphyrin **7**-H_2-Zn and its monomeric subunits **3**-H_2 and **6**-Zn in CH_2Cl_2.

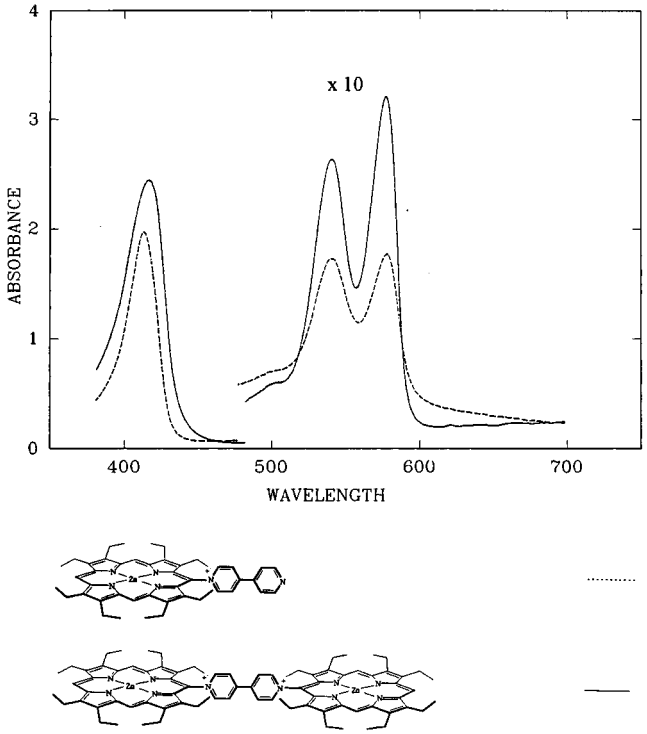

Figure 5. UV−vis absorption spectra of the bisporphyrin **8**-Zn-Zn and the corresponding subunit **6**-Zn in CH_2Cl_2.

substitution site may be determined by the localization energies, and therefore the meso-positions are favored as compared with the β-sites.

UV−Vis Absorption Spectra. Spectra for some of the porphyrins studied here are shown in Figures 4 and 5. Complete UV−vis data are reported in the Experimental Section for the electrosynthesized monomeric and dimeric porphyrins.

Monomers. All the porphyrins synthesized exhibited a red shift of the Soret (B) and visible (Q) bands compared to the corresponding unsubstituted porphyrins. This bathochromic shift resulted from the electron-withdrawing effects[27,28] of the meso- or β-substituent on the porphyrin. The shifts of the Soret bands were comparable (about 15 nm) for β- and meso-substitutions. However, the bathochromic shift of the Q bands was slightly larger with 4,4′-bpy$^+$ than with py$^+$ as expected from the slightly more electron-withdrawing character of 4,4′-bpy$^+$.

Dimers. Their UV−vis absorption spectra (Figure 4) were the mere addition of the spectra of the corresponding monomeric subunits. However, the Soret band of the symmetrical dimer **8**-Zn-Zn showed significant broadening (Figure 5), and its extinction coefficient was ca. one-half of that expected. This result suggested excitonic interactions between the two porphyrin rings in this dimer. Similar spectral effects in dimeric or trimeric porphyrins[29] have been previously reported and analyzed[3d] as dependent on the interporphyrin angles, the direction of the transition dipole moments in the monomer subunits,[30] and also the distances between porphyrins.

Proton NMR Spectra

Monomers. In the monomeric porphyrin **3**-H_2, the pyrrolic protons all appeared down field from those of the phenyl ring, thereby indicating that the aromaticity of the porphyrin ring was not interrupted.[11e] One of the β-proton signals appeared as a singlet at field 9.43 ppm. It corresponded to the proton adjacent to the bipyridinium substituent. The other β-proton signals appeared as two singlets at 9.08 (2H) and 8.96 (1H) ppm plus a multiplet (3H) in the region 8.83−8.77 ppm.

The signals for the phenyl protons were identifiable as ortho, meta, or para on the basis of earlier results[11c,e] or reports on pyridinium-substituted cations. As expected, the internal N-H protons appeared as a singlet at higher field, −2.67 ppm.

The bipyridinium protons appeared at low field, respectively, as two doublets and doubled doublets. With the corresponding zinc-metalated monomer **3**-Zn, the typical adjacent β-H proton signal appeared again at low field (9.30 ppm) as a signature characterizing the mono-β-substitution. The other β-H and bipyridinium proton signals were not as clearly separated as with the unmetalated monomer. All the phenyl protons appeared here as a complex multiplet in the range of 7.99−7.08 ppm.

With the monomers **5**-Zn and **6**-Zn prepared from ZnOEP, ^{1}H NMR observation of two different types of meso-H signals in the range of 10.44−10.34 ppm was fully consistent with the

(27) Hirota, J.; Okura, I. *J. Phys. Chem.* **1993**, *97*, 6867−6870.
(28) Giraudeau, A.; Callot, H. J.; Jordan, J.; Ezahr, I.; Gross, M. *J. Am. Chem. Soc.* **1979**, *101*, 3857−3862.
(29) (a) Sessler, J. L.; Capuano, V. L. *Tetrahedron Lett.* **1993**, *34*, 2287−2290. (b) Osuka, A.; Ikawa, Y.; Maruyama, K. *Bull. Chem. Soc. Jpn.* **1992**, 65, 3322−3330. (c) Wagner, R. W.; Lindsey, J. S. *J. Am. Chem. Soc.* **1994**, *116*, 9759−9760. (d) Prathapan, S.; Johnson, T. E.; Lindsey, J. S. *J. Am. Chem. Soc.* **1993**, *115*, 7519−7520. (e) Seth, J.; Palaniappan, V.; Johnson, T. E.; Prathapan, S.; Lindsey, J. S.; Bocian, D. F. *J. Am. Chem. Soc.* **1994**, *116*, 10578−10592.
(30) (a) Tabushi, I.; Sasaki, T. *J. Am. Chem. Soc.* **1983**, *105*, 2901−2902. (b) Tabushi, I.; Kugimiya, S. I.; Kimmaird, M. G.; Sasaki, T. *J. Am. Chem. Soc.* **1983**, *107*, 4192−4199. (c) Sessler, J. L.; Hugdahl, J.; Johnson, M. R. *J. Org. Chem.* **1986**, *51*, 2838−2840. (d) Won, Y.; Friesner, R. A.; Johnson, M. R.; Sessler, J. L. *Photosynth. Res.* **1989**, *22*, 201−210. (e) Sessler, J. L.; Capuano, V. L.; Harriman, A. *J. Am. Chem. Soc.* **1993**, *115*, 4618−4628.

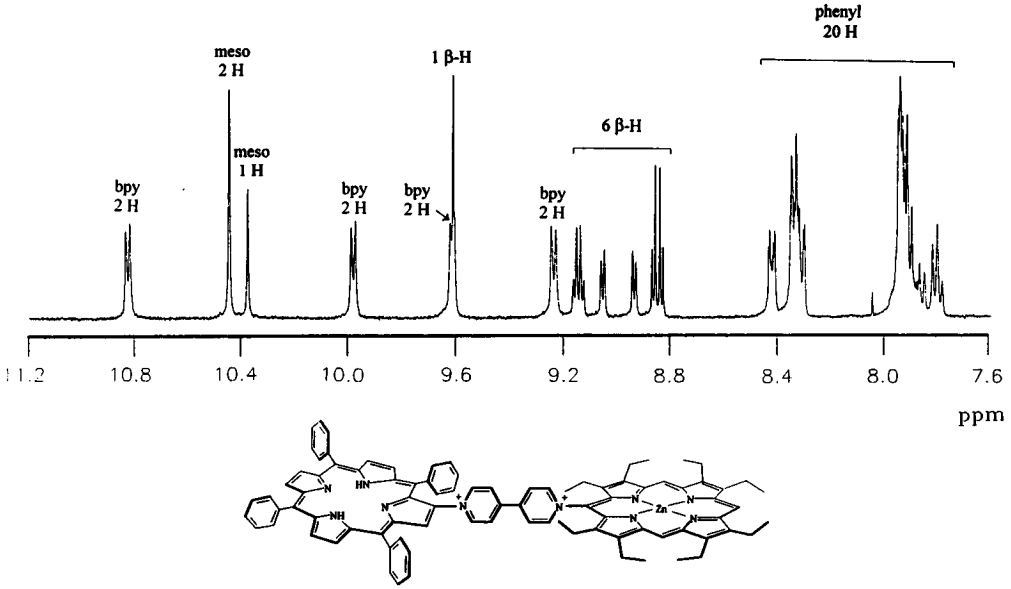

Figure 6. ^{1}H NMR of the bisporphyrin **7**-H_2-Zn (400 MHz, $(CD_3)_2CO$), aromatic region of the spectrum.

proposed meso-substitution.[31] These two singlets which integrated in the ratio 1:2 or 2:1 appear to be diagnostic of transannular monosubstitution on a meso-position. The ethyl proton signals gave a well-separated set of three distinct quartets and triplets in the range 4.21−1.39 ppm. At variance with the expected effect of the electron-withdrawing bpy^+ or py^+ substituents, the protons belonging to the two ethyl groups adjacent to these substituents appeared at higher field than the protons of the other ethyl groups. This result was obtained with all octaethylporphyrins substituted by bpy^+ and py^+. It might be explained by assuming that the protons of the two adjacent ethyl groups underwent a significant shielding. This shielding originated in the positions of these protons, which were located inside the shielding cone of the pyridinic substituent. Thus, in every case the proton nearest the substituent resonated at higher field than the other ones. The chemical shifts induced by the positive charge were similar with the bipyridinium and pyridinium substituents; their proton signals appeared at low field as in the monomer **3**-H_2.

Dimers. The three unsymmetrical dimers **7**-H_2-Zn (Figure 6), **7**-H_2-H_2 and **7**-Zn-Zn gave very well-resolved ^{1}H NMR spectra. The observed ^{1}H NMR signals could be analyzed in two sets: The first one corresponded to the porphyrinic protons and the second one to the viologen protons. As shown with **7**-H_2-Zn and **7**-Zn-Zn complexes, the porphyrinic proton signals could be fairly well described as the addition of those of the corresponding monomers **3**-H_2, **3**-Zn, and **6**-Zn. Only slight chemical shifts were observed. As shown in Figure 7 with the dimers **7**-H_2-Zn and **7**-H_2-H_2, the inner N-H proton signals appeared as a singlet for the TPP subunit, and they split into a well-resolved pair for the OEP subunit. This result suggested that N−H tautomerization was slow in OEP and faster in TPP on the NMR time scale. Such observations have been well documented previously.[32] As seen with the monomers, the viologen proton signals appeared again as four doublets. However, the doublets observed at the higher fields with the singly charged bipyridinium in the monomers appeared now at lower fields due to the double positive charge on the spacer. As clearly demonstrated with the meso-proton signals, the ^{1}H NMR spectrum of the symmetrical dimer **8**-Zn-Zn was the

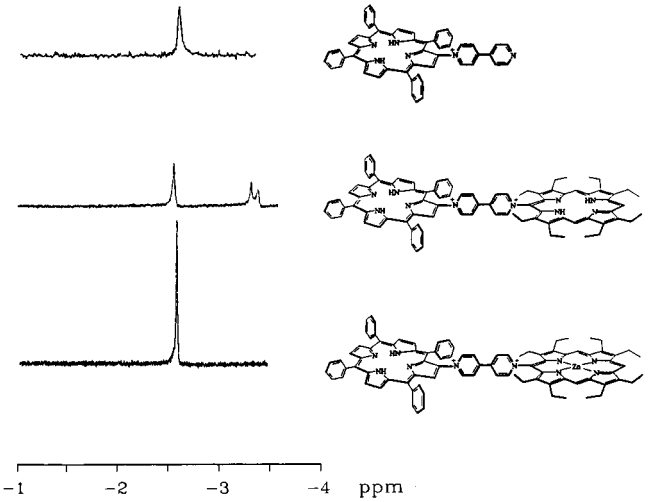

Figure 7. N-H proton signals in the ^{1}H NMR spectra of **3**-H_2, **7**-H_2-H_2, and **7**-H_2-Zn (400 MHz, $(CD_3)_2CO$).

equivalent of twice the corresponding signal of the monomer. This reflected the complete longitudinal symmetry in the molecule. As expected, the four viologen proton doublets of the monomer merged now into two doublets at low field.

Surprisingly, the ^{1}H NMR dimer spectra recorded at 300 K with dilute solutions (10^{-4}−10^{-3} M) did not show any viologen proton signals nor any signal of the β-H proton adjacent to the viologen. Only in concentrated (10^{-3}−10^{-2} M) or saturated solutions are their resonances observed. This lack of signals was examined by variable temperature experiments recorded on diluted solutions and illustrated for the dimer **7**-H_2-Zn in Figure 8. At low temperature, the ^{1}H NMR spectrum was consistent with the spectrum recorded at room temperature in concentrated solutions. All the viologen protons appeared as four doublets. When the sample was warmed, complete flattening was observed in the temperature range 270−280 K. The viologen subunit was conjugated with only one conformational degree of freedom, and the geometry of the molecule could be described, as a first approximation, by the angle

(31) Smith, K. M.; Bobe, F. W.; Minnetian, O. M.; Abraham, R. J. *Tetrahedron* **1984**, *40*, 3263−3272.

(32) (a) Nagata, T. *Bull. Chem. Soc. Jpn.* **1991**, *64*, 3005−3016. (b) Abraham, R. J.; Hawkes, G. E.; Smith, K. M. *Tetrahedron Lett.* **1974**, *16*, 1483. (c) Hobbs, J. D.; Majumder, S. A.; Luo, L.; Sickelsmith, G. A.; Quirke, J. M. E.; Medforth, C. J.; Smith, K. M.; Shelnutt, J. A. *J. Am. Chem. Soc.* **1994**, *116*, 3261−3270.

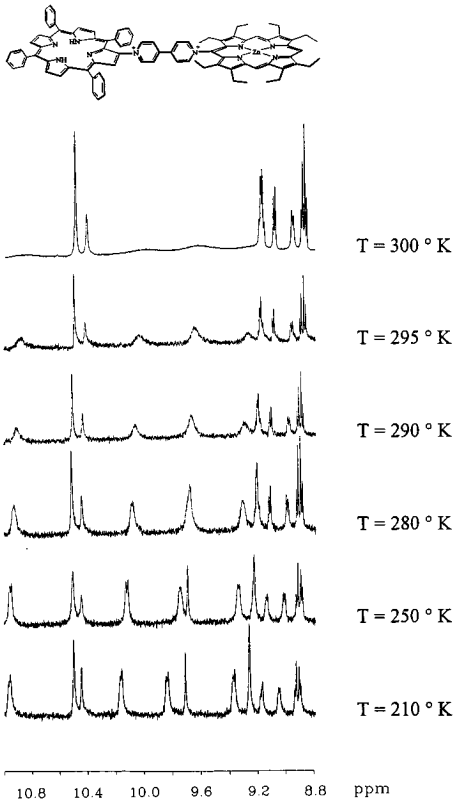

Figure 8. VT−^{1}H NMR study of **7**-H_2-Zn at 400 MHz. Solvent: $(CD_3)_2CO$; 300−210 K.

between the two porphyrin planes. Recent results[6,33] have shown that, in 4,4′-bipyridine complexes, rotation from a planar to a perpendicular conformation causes a decrease of the $\pi-\pi$-electronic coupling between the two porphyrin subunits. Thus, the observed pseudocoalescence might result from a thermally activated rotation between the two porphyrin rings. It is reasonable to speculate that the rotation would also be slowed or hindered by intermolecular Coulombic interactions, which are strongly dependent on the concentration in solution.

Electrochemistry

The electrochemical behavior of free base porphyrins and metalloporphyrins involving nonelectroactive metals is well documented.[19,34] In the potential range of 2 to −2 V, the oxidation and the reduction of the π ring proceed each via two reversible one-electron steps generating radical cations and dications or radical anions and dianions, respectively. The redox behavior of pyridinium[35] and viologen[36] has also been studied in many reports which consistently demonstrated that they were reduced, respectively, in one or two distinct one-electron steps. Electrochemical results are gathered in Table 1. The number of exchanged electrons for each system was determined by exhaustive Coulometry or comparison between the limiting currents of the different waves characterizing a given system.

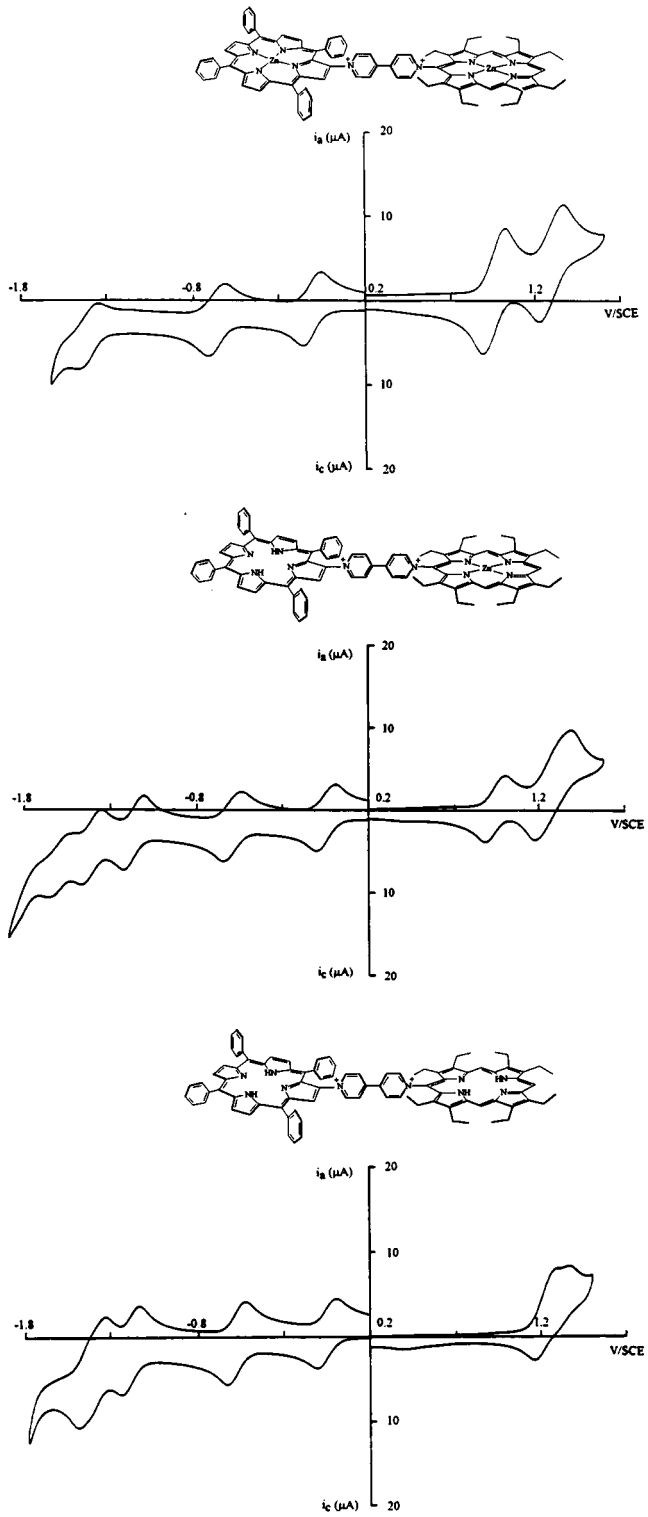

Figure 9. Cyclic voltammograms of **7**-Zn-Zn, **7**-H_2-Zn, and **7**-H_2-H_2 in CH_3CN + 1,2-$C_2H_4Cl_2$ (1/4) + 0.1 M TEAP. Scan rate: $v = 100$ mV s^{-1}. Working electrode: Pt.

The assignment of the sites undergoing the electron transfers was achieved by spectrophotoelectrochemical experiments or comparison of the recorded voltammograms with those of well-known parent compounds and by use of the usual criteria[34b] relative to the redox behavior of the porphyrinic systems. Typical cyclic voltammograms are presented in Figure 9.

Monomers. With the substituted monomers, the known oxidations and reductions of the porphyrin were observed, plus an additional one-electron transfer, corresponding to the reduction of the 4,4′-bpy^+ or py^+ substituent. The measured reduction

(33) Gourdon, A. New *J. Chem.* **1992**, *16*, 953−957.
(34) (a) Fuhrhop, J. H.; Mauzerall, D. *J. Am. Chem. Soc.* **1969**, *91*, 4174−4181. (b) Fuhrhop, J. H.; Kadish, K. M.; Davis, D. G. *J. Am. Chem. Soc.* **1973**, *95*, 5140−5147. (c) Wolberg, A.; Manassen, J. *J. Am. Chem. Soc.* **1970**, *92*, 2982−2991. (d) Antipas, A.; Dolphin, D.; Gouterman, M.; Johnson, E. C. *J. Am. Chem. Soc.* **1978**, *100*, 7705−7709.
(35) (a) Grimshaw, J.; Moore, S.; Thompson, N.; Trocha-Grimshaw, J. *J. Chem. Soc., Chem. Commun.* **1983**, 783−784. (b) Volke, J.; Urban, J.; Volkeova, V. *Electrochim. Acta* **1992**, *37*, 2481−2490.
(36) (a) Elafsen, R. M.; Edsberg, R. L. *Can. J. Chem.* **1957**, *35*, 646−650. (b) Osa, T.; Kuwana, T. J. *Electroanal. Chem.* **1969**, *22*, 389−406. (c) Bard, A. *J. Adv. Phys. Org. Chem.* **1976**, *13*, 155−278. (d) Wüm, G. S.; Berneth, H. *Top. Curr. Chem.* **1980**, *92*, 1−44.

potentials for these reductions, −1.1 V/SCE for 4,4′-bpy$^+$ and −0.65 V/SCE for py$^+$, matched the usual reduction potentials of these cationic species.

The presence of a substituting group induced some changes in the parameters characterizing the electron transfers to or from the porphyrin ring. The oxidation potentials shifted about 150 mV more positive than the oxidation of the corresponding unsubstituted porphyrin. This shift may be ascribed to the electron-withdrawing effect[37] of the positively charged substituent on the π system of the porphyrin. The irreversible two-electron transfer observed with the free bases **2**-H_2 and **3**-H_2 may be explained by the instability and the high reactivity of the radical, resulting from the first electron transfer, which therefore facilitated a second electron transfer.

Dimers. They exhibited three distinct electroactive components, namely, the viologen spacer and the two lateral porphyrins P_1 and P_2. The viologen (4,4′-bpy)$^{2+}$ was reduced in two distinct steps, each being a reversible one-electron reaction as is well known for the viologens.[36]

As expected for viologen bearing electron-rich substituents, these reductions occurred easily at low potentials. Meanwhile, the porphyrins P_1 and P_2 remained unaffected by these electron transfers. The measured potentials of the viologens in the series of dimers also indicated that their first and second reductions became more difficult when the net ring charge[34b] increased on the substituting porphyrins P_1 and P_2: The reduction potentials of the viologen became more negative in the sequence **7**-H_2-H_2 < **7**-Cu-Cu < **7**-H_2-Zn < **7**-Cu-Zn < **7**-Zn-Zn. This result matched the sequence proposed by Fuhrhop and Kadish[34b] for the electronegativity of porphyrins.

The electrochemical oxidations and reductions of the porphyrins P_1 and P_2 occurred on both sides of the electroactivity range of the spacer. As a rule, these charge transfers on P_1 and P_2 were one-electron reversible processes. Some of them, which appeared as reversible two-electron transfers, actually resulted from the merging of two distinct one-electron steps. In these porphyrins P_1 and P_2, the observed electron transfers were easily assigned to the π systems of the OEP or TPP, based on the potentials measured for the corresponding bipyridinium-substituted monoporphyrins. This assignment was also achieved by use of known general redox characteristics[34,37−40] of the porphyrins. The electrochemical oxidation of the porphyrin dimers was monitored by spectroelectrochemistry (Figure 10). The first oxidation revealed a decrease in the intensity of the Soret band, as usually observed[19,34,41] in the generation of porphyrin cation radicals. The oxidized porphyrin reverted quantitatively to the initial dimer on the reverse potential scan (Figure 10a). The reduction reactions were more complex. Although cyclic voltammetry indicated that the first reduction was reversible, the electrogenerated species were not stable on longer time scales. Spectroelectrochemistry indicated that the first reduction produced radical anions and the expected weakening of the Soret band. However, the return scan

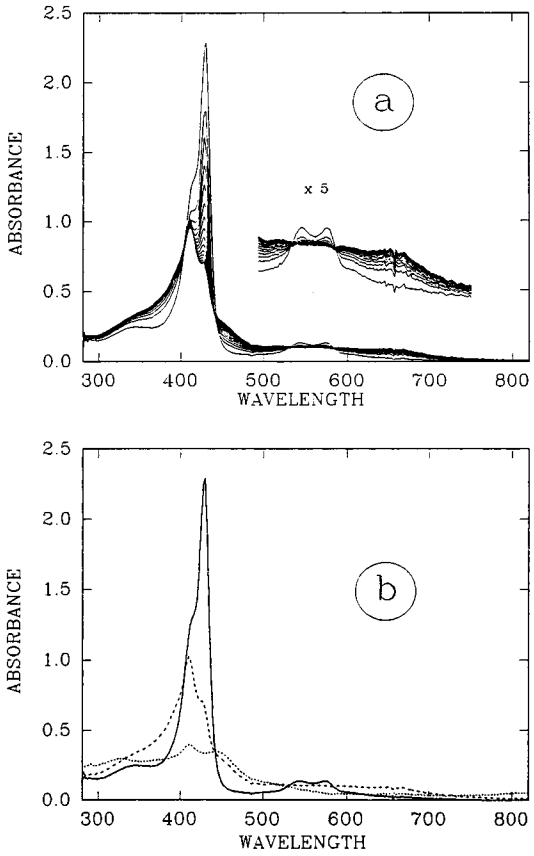

Figure 10. (a) UV−vis absorption spectra recorded during the oxidation of **7**-Zn-Zn in CH_3CN/1,2-$C_2H_4Cl_2$ (1/4) and 0.1 M TEAP at −1.1 V/SCE. (b) UV−vis absorption spectra of **7**-Zn-Zn: (—) unoxidized form, (− − −) two-electron-oxidized species (first wave, 0.95 V), and (···) four-electron-oxidized species (second wave, 1.27 V).

generated only a fraction of the initial dimer. Thus, the dimers seemed more stable in the oxidized state than in the reduced state, as already observed for the monomers. The strikingly close values observed between the reduction potentials of the dimers and those of the monomers or the initial porphyrin components could be expected because the reduction of the dimers actually occurred on neutral molecules, the 4,4′-bpy^{2+} becoming neutral (via two one-electron reductions) before the reductions of the porphyrins P_1 and P_2. The symmetrical dimer **8**-Zn-Zn was oxidized via two steps each involving two electrons and could be described as noninteracting redox centers[42] under the conditions of the experiment.

ESR. As reported above, ^{1}H NMR results on concentrated solutions of dimers indicated that hindered rotation was possible for one porphyrin with respect to the second one in the dimers. Hence, the existence of possible inter- or intramolecular interactions in these dimers should be considered. We have therefore synthesized porphyrin dimers containing one or two divalent copper ions, namely, **7**-Cu-Zn and **7**-Cu-Cu. In such molecules, the paramagnetic copper served as a good sensor for the existence of metal−metal interactions. With this aim, the magnetic susceptibility ($\chi = f(T)$) of the dimeric **7**-Cu-Cu solid was studied. The values of χ were obtained by double integration of the ESR signal characteristics of Cu(II) in the porphyrin dimer. Recent ESR results[43] for a planar biscopper^{II} phthalocyanine yielded a 96 G peak-to-peak signal, which

(37) (a) Kadish, K. M.; Morrison, M. M. *Inorg. Chem.* **1976**, *15*, 980−987. (b) Giraudeau, A.; Louati, A.; Gross, M.; Callot, H. J.; Hanson, L. K.; Rhodes, R. K.; Kadish, K. M. *Inorg. Chem.* **1982**, *21*, 1581−1586.

(38) (a) Felton, R. H.; Linschitz, H. *J. Am. Chem. Soc.* **1966**, *88*, 1113−1116. (b) Truxillo, L. A.; Davis, D. G. *Anal. Chem.* **1975**, *47*, 2260−2266.

(39) (a) Kadish, K. M.; Davis, D. G. *Ann. N. Y. Acad. Sci.* **1973**, *206*, 495−502. (b) Kadish, K. M.; Morrison, M. M. *J. Am. Chem. Soc.* **1976**, *98*, 3326−3328.

(40) Giraudeau, A.; Callot, H. J.; Gross, M. *Inorg. Chem.* **1979**, *18*, 201−206.

(41) (a) Malinski, T.; Chang, D.; Latour, J. M.; Marchon, J. C.; Gross, M.; Giraudeau, A.; Kadish, K. M. *Inorg. Chem.* **1984**, *23*, 3947−3944. (b) Kadish, K. M.; Dubois, D.; Barbe, J. M.; Guilard, R. *Inorg. Chem.* **1991**, *30*, 4498−4501. (c) Kadish, K. M.; Han, B. C.; Endo, A. *Inorg. Chem.* **1991**, *30*, 4502−4506.

(42) Hammel, D.; Erk, P.; Schuler, B.; Heinze, J.; Müllen, K. *Adv. Mater.* **1992**, *11*, 737−739.

(43) Lelièvre, D.; Bosio, L.; Simon, J.; André, J. J.; Bensebaa, F. *J. Am. Chem. Soc.* **1992**, *114*, 4475-4479.

indicated a significant dipolar coupling. On the other hand, the magnetic susceptibilities (χ) measured at various temperatures revealed the existence of both ferromagnetic intermolecular and antiferromagnetic intramolecular interactions.

In the porphyrin dimer **7**-Cu-Cu, the ESR spectra exhibited a peak-to-peak $W_{pp} = 95$ G, thus indicating the occurrence of strong intermolecular dipolar coupling. The low value obtained for g (=2.066) indicated that the spin−orbit coupling was higher in **7**-Cu-Cu than in the above-cited biscopper^{II} phthalocyanine ($g = 2.048$). Hence, the unpaired electron was more localized on the copper in **7**-Cu-Cu than in the biscopper phthalocyanine. The plot $\chi(T)$ showed that in the dimer **7**-Cu-Cu the susceptibility obeyed a Curie−Weiss relationship ($\chi = C/(T - T_c)$) in which $T_c = 7.1$ K (T_c = coupling temperature). Although the peak-to-peak field broadened slowly with temperature (from 96 G at 300 K to 110 G at 4 K), this broadening indicated that a ferromagnetic intermolecular interaction existed, although weak. Actually, the exchange interaction energy was estimated as 0.6 meV ($J = k_B T_c$ for an assumed one-dimension cubic stacking). The dimer **7**-Cu-Zn was also studied by ESR under the same conditions as **7**-Cu-Cu. The obtained spectrum exhibited a hyperfine structure due to the copper(II) ($S = 3/2$). This hyperfine structure resulted from a dilution effect of the copper porphyrins, as the second metal (Zn) was diamagnetic in the dimer. In this dimer, **7**-Cu-Zn, the plot $\chi(T)$ revealed, as in the dimer **7**-Cu-Cu, a ferromagnetic interaction with $T_c = 4.8$ K.

These ESR results obtained on solid dimers therefore indicated the absence of intramolecular copper−copper interactions (in **7**-Cu-Cu) and the occurrence of a copper−copper ferromagnetic coupling in both dimers **7**-Cu-Zn and **7**-Cu-Cu. ESR experiments carried out with solutions of these dimers did not produce additional information.

Conclusion

A new method has been reported allowing the synthesis of porphyrin dimers by controlled potential electrolysis. The generated species have been identified. This method was based on a nucleophilic substitution carried out on two electrooxidized porphyrins. It allowed the two-step synthesis of symmetric dimers (OEP−OEP) and asymmetric dimers (TPP−OEP) with good yield (>50%). It was also demonstrated that each of the two substitution steps was accounted for by a two-electron $E_1C_NE_2C_B$ mechanism. In the ^{1}H NMR spectra of the **7**-H_2-Zn porphyrin dimer, the lack of signals typical of the bridging viologen protons and the β-H protons adjacent to the viologen provided evidence of rotation at the juncture of the TPP unit with the viologen spacer and also between the two pyridinium subunits of the spacer. UV−vis spectrum of the symmetric dimer **8**-Zn-Zn showed the presence of excitonic interactions between the porphyrin subunits. The ESR analysis indicated that an intermolecular ferromagnetic coupling occurred between copper atoms.

The redox characteristics of the studied monomers and dimers revealed, in all these molecules, that the oxidation and reduction potentials of the porphyrin subunits flanked both sides of the electroactive range characterizing the spacer. The electron-withdrawing character of the latter was quantitated through the anodic shift of the first-oxidation potential of the porphyrin component(s). The monomers provided experimental evidence that their first oxidation produced stable porphyrin radical cations only when metalated. Also their reduction mechanism was complex, probably because the reduced bipyridinium cation was not stable. The dimers exhibited an electrochemical behavior of their porphyrin components that was close to that of the corresponding monomers. All the redox parameters recorded on the studied molecules consistently indicated that their subunits (i.e., porphyrin(s) and spacer) were almost noninteracting under the present experimental conditions.

The synthetic method reported here is the first method allowing electrochemical synthesis of porphyrin dimers. It opens a new avenue to the preparation of diverse porphyrin derivatives, through appropriate selection of the porphyrin subunits and the spacer. Hence, further studies now become possible on ad-hoc assemblies of chromophoric subunits. Such studies are of major interest for further understanding the interactions and the charge transfers between these subunits and ultimately for effectively replicating photosynthetic pathways or creating new materials.

Experimental Section

Materials. All solvents and chemicals were of reagent grade quality, purchased commercially, and used without further purification except as noted below. CH_2Cl_2 and $CHCl_3$, for use in exhaustive electrolysis, were heated at reflux with and distilled from CaH_2. The supporting electrolyte tetraethylammonium perchlorate (TEAP) was purified as previously described.[28] Complex **4**-Zn was purchased from Aldrich Chemical Co. Thin layer chromatography (TLC) was performed on commercially prepared alumina or silica gel plates purchased from Roth Sochiel.

Apparatus. All electrochemical measurements were carried out under argon. Voltammetric data were obtained with a standard three-electrode system using a Bruker E 130 M potentiostat and a high-impedance millivoltmeter (Minisis 6000, Tacussel). Current−potential curves were obtained from an Ifelec If 3802 X-Y recorder. The working electrode was a platinum disk (EDI type, Solea Tacussel) of 3.14 mm^2 surface area. A platinum wire was used as the auxiliary electrode. The reference electrode was a saturated calomel electrode (SCE) that was electrically connected to the studied solution by a junction bridge filled with the corresponding solvent-supporting electrolyte solution.

Coulometric measurements and quantitative electrochemical synthesis were performed in either a standard 50 mL cell or a large 850 mL cell. In the standard cell, the working electrode was a platinum wire (o.d. = 0.8 mm) of 60 cm length. In the large cell, the working electrode was a cylindric platinum grid (o.d. = 5 cm, height = 7 cm). For the controlled-potential electrolysis, the anodic and cathodic compartments were separated by a fritted glass disk to prevent diffusion of the electrogenerated species.

The spectrophotometric analyses were performed with a Hewlett-Packard 8452 A diode array spectrometer. The thin layer spectroelectrochemical cell has been previously described.[44]

UV−vis spectra were recorded on a Shimazu UV-260 spectrophotometer. ^{1}H NMR spectra were obtained in $CDCl_3$ or $(CD_3)_2CO$ on Bruker AM-400 (400 MHz), AC 300 (300 MHz), and WP 200 (200 MHz) spectrometers. Fast atom bombardment mass spectra (FAB-MS) were obtained using a 3-nitrobenzyl alcohol (NBA) matrix on a FAB-HF mass spectrometer. Elementary analyses were performed by the microanalysis services of Institut Charles Sadron or Chemical Department of IUT Sud (Strasbourg). ESR spectra were recorded at X-band frequencies on a Bruker ESP 300 spectrometer equipped with a variable temperature accessory.

Synthesis. Compounds **1**-H_2 and **1**-Zn were prepared and purified by known procedures.[45,46] Compounds **2**-H_2 and **2**-Zn have been previously reported.[12,14]

Electrochemical Synthesis: General Procedure. Prior to electrolysis, the corresponding mixtures were stirred and degassed by bubbling argon through the solution for 10 min. Then, the desired working potential was applied. During anodic oxidation, the electrolyzed solution was continuously stirred and maintained under argon.

(44) Bernard, C.; Gisselbrecht, J. P.; Gross, M.; Vogel, E.; Lausmann, M. *Inorg. Chem.* **1994**, *33*, 2393−2401.

(45) (a) Adler, A. D.; Longo, F. R.; Finarelli, J. D.; Goldmacher, J.; Assour, J.; Korsakoff, L. *J. Org. Chem.* **1967**, *32*, 476. (b) Barnett, G. H.; Hudson, M. F.; Smith, K. M. *Tetrahedron Lett.* **1973**, *30*, 2887−2888.

(46) Adler, A. D.; Longo, F. R.; Kampas, F.; Kim, K. J. *Inorg. Nucl. Chem.* **1970**, *32*, 2443−2445.

After electrolysis, solvents were removed by rotary evaporator. The residue was dissolved in a minimum of CH_2Cl_2; then the mixture was poured into water, and the organic layer was washed twice. Typical preparation and characterization of a substituted monomer (**3**-H_2) and a dimer (**7**-H_2-Zn) are reported hereafter.

3-H_2. H_2TPP (30 mg, 0.049 mmol) and 150 mg of 4,4′-bipyridine (0.960 mmol) were dissolved in 25 mL of a $CHCl_3/CH_3CN$ (4/1) and 0.1 M TEAP. solution. The electrolysis was carried out during 3 h at 1.05 V/SCE. After treatment, the organic extract was concentrated (∼10 mL) and chromatographed on alumina. The first fraction (eluted with CH_2Cl_2) was unreacted H_2TPP. The desired product was eluted with a mixture of CH_2Cl_2/CH_3OH (98/2). After evaporation of the solvent, **3**-H_2 was recrystallized from CH_2Cl_2/*n*-hexane to give violet-blue crystals (40 mg, yield 94%). **3**-H_2 was dried under vacuum at 120 °C during 24 h.

By the same procedure, anodic oxidation of 980 mg of H_2TPP (1.6 mmol) in the presence of 5 g of 4,4′-bipyridine (32 mmol) in a 850 mL solution of the supporting electrolyte gave **3**-H_2 with a yield of 75% after 48 h of electrolysis: UV−vis (CH_2Cl_2) λ_{max} (nm) (ϵ, M^{-1} cm^{-1}) 422 (258 700), 526 (15 200), 564 (2400), 602 (4300), 658 (9200); ^{1}H NMR (200 MHz, $(CD_3)_2CO$) δ 9.58 (d, J_o = 7 Hz, 2 H, 4,4′-bpy$^+$), 9.43 (s, 1 H, β-H adjacent to 4,4′-bpy$^+$), 9.08 (s, 2 H, β-H), 8.96 (s, 1H, β-H), 8.98 (dd, J_o = 4.4 Hz, J_m = 1.7 Hz, 2H, 4,4′-bpy$^+$), 8.83−8.77 (m, 3 H, β-H), 8.48 (d, J_o = 7 Hz, 2 H, 4,4′-bpy$^+$), 8.34−8.22 (m, 6 H, o-H), 8.13 (dd, J_o = 4.7 Hz, J_m = 1.6 Hz, 2 H, o-H of Ph adjacent to 4,4′-bpy$^+$), 8.05 (dd, J_o = 4.4 Hz, J_m = 1.7 Hz, 2 H, 4,4′-bpy$^+$), 7.90−7.81 (m, 9 H, m- and p-H), 7.52−7.49 (m, 3 H, m- and p-H of Ph adjacent to 4,4′-bpy$^+$), −2.67 (s, 2 H, NH); FAB-MS (NBA) m/z = 769.2 $(C_{54}H_{37}N_6)^+$. Anal. Calcd. for $C_{54}H_{37}N_6ClO_4$: C, 74.60; H, 4.29; N, 9.67; Cl, 4.08. Found: C, 74.31; H, 4.34; N, 9.49; Cl, 4.25.

7-H_2-Zn. ZnOEP (220 mg, 0.37 mmol) and 643 mg of **3**-H_2 (0.74 mmol) were dissolved in 850 mL of a 1,2-$C_2H_4Cl_2/CH_3CN$ (4/1) and 0.1 M TEAP mixture. The electrolysis was carried out at 0.70 V/SCE during 48 h. After treatment the organic extract was chromatographed on a silica gel column (Kieselgel, 230−400 mesh). The first fraction (elution with CH_2Cl_2) gave unoxidized ZnOEP. The second bluish-purple fraction (unreacted **3**-H_2) was collected by elution with CH_2Cl_2/CH_3OH (98/2). Further elution with CH_2Cl_2/CH_3OH (96/4) gave the dimer **7**-H_2-Zn. After evaporation of the solvent, **7**-H_2-Zn was recrystallized from CH_2Cl_2/*n*-hexane to give black-violet crystals (428 mg, 0.27 mmol, yield 73%): UV−vis (CH_2Cl_2) λ_{max} (nm) (ϵ, M^{-1} cm^{-1}) 406 (176 200), 424 (416 600), 536 (24 000), 577 (20 800), 656 (8000); ^{1}H NMR (400 MHz, $(CD_3)_2CO$) δ 10.83 (d, J_o = 6.4 Hz, 2 H, 4,4′-bpy^{2+}), 10.44 (s, 2 H, meso-H), 10.37 (s, 1 H, meso-H), 9.97 (d, J_o = 6.6 Hz, 2 H, 4,4′-bpy^{2+}), 9.60 (d, J_o = 6.4 Hz, 2 H, 4,4′-bpy^{2+}), 9.60 (s, 1 H, β-H adjacent to 4,4′-bpy^{2+}), 9.22 (d, J_o = 6.6 Hz, 2 H, 4,4′-bpy^{2+}), 9.11 (d, J_{cis} = 5 Hz, 1 H, β-H), 9.10 (d, J_{cis} = 5 Hz, 1 H, β-H), 9.03 (d, J_{cis} = 5 Hz, 1 H, β-H), 8.91 (d, J_{cis} = 5 Hz, 1 H, β-H), 8.84 (d, J_{cis} = 4.7 Hz, 1 H, β-H), 8.81 (d, J_{cis} = 4.7 Hz, 1 H, β-H), 8.39 (dt, J_o = 7.6 Hz, J_m = 2.1 Hz, 2 H, o-H of Ph adjacent to 4,4′-bpy^{2+}), 8.32−8.27 (m, 6 H, o-H of Ph), 7.91−7.75 (m, 12 H, m- and p-H), 4.20 (q, ^3J = 7.5 Hz, 12 H, 6 CH_2 of -CH_2-CH_3), 2.79 (q, ^3J = 7.4 Hz, 4 H, 2 CH_2 of -CH_2-CH_3), 1.97 (t, ^3J = 7.5 Hz, 18 H, 6 CH_3 of -CH_2-CH_3), 1.59 (t, ^3J = 7.4 Hz, 6 H, 2 CH_3 of -CH_2-CH_3 adjacent to 4,4′-bpy^{2+}), −2.59 (s, 2 H, NH of TPP); FAB-MS (NBA) m/z = 1564.5 $(C_{90}H_{80}N_{10}Zn(ClO_4)_2^+)$, 1465.5 $(C_{90}H_{80}N_{10}Zn(ClO_4)^+)$, 1366.6 $(C_{90}H_{80}N_{10}Zn^+)$, 683.2 $(C_{90}H_{80}N_{10}Zn^{2+})$. Anal. Calcd. for $C_{90}H_{80}N_{10}Zn(ClO_4)_2$: C, 69.03; H, 5.15; N, 8.94; Cl, 4.53; Zn, 4.18. Found: C, 68.90; H, 4.99; N, 8.90; Cl, 4.75; Zn, 4.20.

Acknowledgment. We warmly thank the Centre National de la Recherche Scientifique for financial support. We express our gratitude to Professor J. Fajer for helpful discussions and critical comments. We are also grateful to Drs. J. J. Andre and C. Haubtmann, Institut Charles Sadron (UP au CNRS No. 0022), for the ESR studies.

Supporting Information Available: Procedures for the preparation of and selected physical data for compounds **3**-Zn, **5**-Zn, **6**-Zn, **7**-H_2-H_2, **7**-Zn-Zn, **7**-Cu-Cu, **7**-Cu-Zn, and **8**-Zn-Zn. Also lists of ESR spectra and UV−vis spectra (10 pages). This material is contained in many libraries on microfiche, immediately follows this article in the microfilm version of the journal, can be ordered from the ACS, and can be downloaded from the Internet; see any current masthead page for ordering information and Internet access instructions.

JA9523956